LA-UR- 97-56

CONF-970126--12

Approved for public release; distribution is unlimited.

Title: USING NAI DETECTORS FOR TOMOGRAPHIC GAMMA SCANNING

Author(s): Robert J. Estep, NIS-6
Sheila Melton, ORNL

MASTER

Submitted to: 5th Nondestructive Assay and Nondestructive Examination Waste Characterization Conference

Salt Lake City UT

January 14-16, 1997

DISCLAIMER

Los Alamos
NATIONAL LABORATORY

DISTRIBUTION OF THIS DOCUMENT IS UNLIMITED

USING NAI DETECTORS FOR TOMOGRAPHIC GAMMA SCANNING

Robert J. Estep and Sheila Melton
Los Alamos National Laboratory, Los Alamos, NM 87545

ABSTRACT

We examined two approaches for using NaI detectors to perform transmission corrections used in the tomographic gamma scanner (TGS) and segmented gamma scanner (SGS) nondestructive assay methods. We found that a material-basis-set (MBS) fit using empirical logarithmic response spectra is quite accurate. Because this is a gross count technique, it gives sensitivities (for equal numbers of detectors) that are roughly ten times better than those obtained using Germanium detectors. We also found that simple continuum subtraction can be used in MBS fits using the energy-group-analysis technique only when the Pu transmission is greater than 10%. Both approaches for using NaI detectors require a knowledge of the Pu (or other) isotopics to obtain full accuracy.

INTRODUCTION

The objective of this study was to develop analysis methods that will allow arrays of NaI and other room-temperature gamma-ray detectors to be used in the tomographic gamma scanner (TGS)[1] and segmented gamma scanner (SGS) methods in place of high-purity-Germanium (HPGe) detectors. NaI detectors are widely used in detector arrays for medical and industrial imaging because of their low cost and simple operation, but they have not been used in TGS and other transmission-corrected gamma-ray nondestructive assay (NDA) methods because the poor energy resolution of NaI complicates analysis and introduces large statistical errors in measurements of continuum-subtracted (net) peak areas. Specifically, neither the ^{75}Se nor the Pu peaks used historically in SGS can be resolved in a NaI spectrum.

In this study we examine data analysis techniques for both the transmission and emission parts of TGS and SGS assays. One of the methods studied applies transmission corrections to gross Pu spectra from NaI detectors. The use of gross counts instead of net counts dramatically improves the sensitivity of TGS assays, as is shown in Table I below.

The table lists estimated low-burnup Pu assay sensitivities (at the 10%, or 0.1 sigma, error level) in a 30-minute emission scan for a TGS system with a varying number of NaI or HPGe detectors. The net area sensitivity estimates are based on a standard one-ROI linear continuum subtraction, while the gross count sensitivities are for assays using the total counts in the 332- to 452-keV peak group of Pu. It can be seen from the table values that the sensitivity using gross count methods with NaI detectors will be about ten times better than that for HPGe detectors using net area methods. In particular, a 120-detector NaI system using gross count methods would have the same sensitivity (5 mg of low-burnup Pu) as the differential dieaway technique.

TABLE I. Estimated TGS Pu 10% sensitivities* for various array sizes

Number of detectors	HPGe net area sensitivity (mg Pu)	NaI net area sensitivity (mg Pu)	NaI gross count sensitivity (mg Pu)
1	600	1200	50
20	132	260	10
40	96	192	8
60	78	160	7
80	66	130	6
120	55	110	5

* estimates are for a non-attenuating matrix with a moderately high ambient background

EXPERIMENTAL DETAILS

To evaluate the effectiveness of the data analysis techniques considered here we performed transmission measurements on a series of attenuating materials. For each absorber we separately measured transmitted spectra from a 100-g metallic low-burnup Pu source, a ^{133}Ba source, a ^{137}Cs source, and a ^{60}Co source using a Bicron 2M2/2 (2-inch diameter by 2-inch thickness) NaI detector and a 35% Ortec GEM-type coaxial HPGe detector. This transmission source combination was recently shown[2] to be optimal for TGS assays of Pu. We then applied different analysis techniques to see how well the transmission data could be used to correct the Pu data for attenuation through the

absorbers. As is discussed below, the effectiveness of an analysis technique in estimating attenuation corrections in this simple geometry can be a good measure of its effectiveness in the TGS or SGS methods.

Table II lists the series of absorbers used. Also shown are the transmission values for the ^{239}Pu 414-keV gamma ray as measured using an HPGe detector as well as the gross count transmission of the 332- to 452-keV group of Pu peaks as measured with the NaI detector. The gross count Pu transmissions are influenced by geometric details that do not affect the 414-keV transmission measured using the HPGe detector. Side scattering of divergent gamma rays back into the detector is the most significant effect. It is observable with every absorber except those of Pb, and is particularly pronounced with the 10-inch polyethlylene absorber. That large-area absorber was composed of a stack of 2-inch-thick polyethlylene blocks with widths varying from 12 to 18 inches. The 4-inch polyethylene absorber, in contrast, was 4- by 6-inches in width, and shows correspondingly less side scattering.

TABLE II. Absorbers Used in Transmission Measurements

Absorber	414-keV transmission (HPGe)	332- to 452-keV gross transmission (NaI)
0.5" stainless steel	.400	.588
1" stainless steel	.156	.315
1" Cu	.162	.317
0.5" Al	.719	.861
1" Al	.521	.725
1.75" Al	.331	.547
0.25" Cd	.564	.614
0.5" Pb	.0534	.0405
10" polyethylene	.0671	.201
air (no absorber)	1.00	1.02
4" polyethylene	.352	.511
0.25" Pb	.225	.199
4" polyethylene plus 0.25" Pb	.0765	.101

To make transmission measurements we placed the NaI and HPGe detectors side by side facing the transmission source. The transmission source position was 18 inches from the detector faces. The absorbers were placed between the source and the detector. Some absorbers were placed closer to the detector, some closer to the source. For a given absorber we used the same placement with each transmission source so that side scatter and other geometric effects would be approximately the same. Using two detectors this way introduced a parallax difference of about 0.6% in the absorber thickness across the detector diameters, which we consider to be negligible.

A second set of absorbers composed of alternating layers of polyethylene and 1/16-inch Pb foils was used to construct empirical basis spectra for the response function methods discussed below. We used transmission spectra for 10 inches of polyethylene and 0.5 inches of Pb as basis spectra in a 2-element material basis set[3] (MBS) approach. To determine the average spectrum shape of the side-scattered gamma rays we collected transmission spectra through the same absorber in configurations that alternately minimized and maximized side-scattering effects. We then subtracted the minimum-scattering spectrum from the maximum-scattering spectrum. As has been observed elsewhere, the shape of this scattered spectrum is fairly constant. Scattering spectra for several absorber combinations were averaged to create a composite scattering spectrum to be used as a response function. This approach characterizes only the excess scattering over the minimum observed; the minimum scattering cases still contain significant scattered counts, as is shown by the transmission values in Table II. Side scattering was characterized only for the ^{133}Ba and the Pu sources.

For measurements with all sources except ^{60}Co we used a weak ^{60}Co rate loss source to normalize spectra and eliminate rate loss effects. A weak ^{137}Cs source was used as the rate loss source for ^{60}Co transmission measurents. Note that we are not recommending the use of rate-loss sources with NaI arrays in general, as they limit the sensitivity in high-efficiency counting applications. All NaI spectra were normalized to the rate-loss peaks by spectrum stripping. Because we used the transmission sources

separately instead of in combination, the stripping procedure produced clean spectra containing only counts from the transmission source.

ANALYSIS METHODS

We used two basic approaches for analyzing NaI spectra: 1) a method based on linear continuum subtraction to obtain net peak areas, and 2) an MBS empirical response-function method. Empirical or theoretical response-function or other peak-fitting methods could be used to extract net full-energy-peak areas from NaI spectra with better accuracy than can be obtained using linear continuum subtraction. We have chosen not to study those refined methods at this time. The response function technique described here is not aimed at obtaining net peak areas, but rather at obtaining gross count corrections. Aside from the elimination of excess side-scattering and emission components in the transmission spectra, the technique is fundamentally non-subtractive. Thus, what we are really comparing is a net area method and a gross count method.

In the simple experiments described here the Pu source represents the emission part of a TGS scan and the other sources the transmission part. We used the MBS method in both approaches to convert attenuation corrections from the transmission to the emission part of the problem. That is, we used the transmission data to compute partial density values (ρ_z) in a basis set of CH_2 and Pb, then we used the ρ_z values to compute attenuation corrections for the emission (Pu) attenuation loss. It is this intermediate conversion to the MBS that allows us to generalize from the simple source→absorber→detector geometry to the TGS geometry, in which a potentially large number of separate sources are mixed randomly with a potentially large number of separate absorbers. Not all methods that work with the simple geometry can be applied to TGS. For example, with the simple geometry one can use a response function technique to estimate the attenuation loss of the Pu source using just the Pu spectrum, eliminating the need for the transmission sources. This approach, however, can not be generalized to TGS.

The analysis of NaI spectra can be greatly simplified by keeping the spectra as pure as possible. We recommend using the different transmission sources separately in different detector planes of the (linear) array. That is, the ^{133}Ba source transmission should be measured by one set of detectors, the ^{137}Cs source by another, and the ^{60}Co source by a third. Throughput can be maintained if the individual sources are each as strong as the single mixed source they replace. Emission gamma rays will contaminate the transmission spectra, so it is prudent with NaI detectors to perform emission measurements at every position used in the transmission scan so that the Pu or other emission spectrum can be stripped from the transmission source spectra.

If a rate loss source is used (as it is here), then its spectrum must also be stripped. Stripping a rate-loss-source spectrum will automatically strip the room background spectrum. If a rate-loss source is not used, then the room background must be stripped from every spectrum. Note that if region-of-interest (ROI) sum techniques are used, the channel-by-channel stripping of spectra can be replaced by a subtraction of ROI sums.

The data-fitting techniques used in this study are implemented in the LANL-developed TGS_FIT[4,5] image reconstruction software, which was used for the MBS, energy-group-analysis, and response-function fitting described below.

NET PEAK AREA METHODS

Figure 1 compares a gamma-ray spectrum of a mixture of ^{133}Ba, ^{137}Cs, and ^{60}Co taken with the HPGe detector to a spectrum taken with the NaI detector. One can see why NaI detectors are shunned in many applications: their energy resolution is 30-40 times worse than that of HPGe detectors. The four ^{133}Ba gamma-rays are easily resolved in the HPGe spectrum and can be separately measured and used as data for fitting MBS or Z-effective attenuation curves. They are not resolved in the NaI spectrum and cannot be separately measured. However, because of the wide energy separation between gamma-

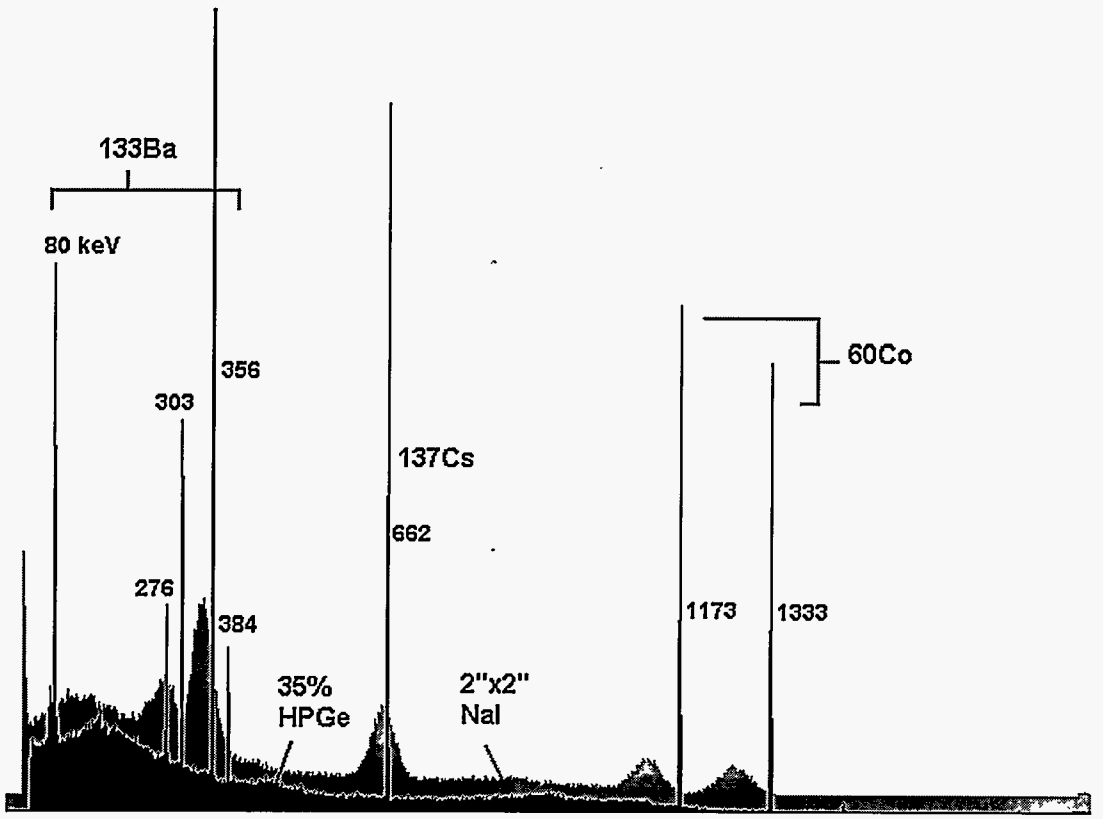

Figure 1. Comparison of HPGe- and NaI spectra of a mixture of ^{133}Ba, ^{137}Cs, and ^{60}Co. Note the wide spacing between the groups of gamma rays emitted by these isotopes.

rays from the three isotopes, it is easy to resolve the ^{133}Ba gamma rays as a group from those emitted by ^{137}Cs and ^{60}Co. Also, the sum of the four ^{133}Ba gamma rays can be measured (approximately) from the NaI spectrum. Since the transmission values of all the transmission gamma rays must lie on the same monotonic attenuation curve, one might intuitively guess that the wide spacing and resolvability of the broad "energy groups" of gamma rays could be used to arrive at a good estimate of the individual gamma-ray intensities within the groups. This is in fact the case, and is the basis for what we are calling the energy-group-analysis method.

Energy-group analysis

The summed intensity of a group of gamma rays of different energies will not obey Beer's attenuation law and so cannot be used directly for transmission imaging or for attenuation-curve fitting with the linear MBS method. However, we have developed an iterative procedure that allows the relative intensities of the individual gamma-rays in a group to be determined at each view. An initial guess is made of the relative transmissions of the gamma rays in the group, and these values are used along with the transmissions of the other energy groups to find an approximate MBS attenuation curve. The attenuation curve is used to make an improved guess of the transmissions, which are then used to make a second, improved MBS fit. This is repeated for a total of five iterations. The rapid convergence of this method is illustrated in figure 2, which shows the attenuation curve for 0.25-inch of cadmium as fitted to the measured transmissions from a ^{133}Ba and ^{137}Cs transmission source combination. Even with a crude initial guess of the individual gamma-ray transmissions (i.e., all transmissions equal), the second estimate is already very close to the correct value.

Once the attenuation curve is known, applying an attenuation correction to a group of unresolved emission gamma-rays is straightforward, provided that the isotopic composition of the emitting source mixture is known. In TGS, for each energy in the emission group one sums the attenuation-corrected emission matrices, $F(E_i)$, for the individual gamma-ray energies E_i, to obtain the group-sum attenuation-corrected emission matrix, F(group). The group matrix is used to reconstruct the ^{239}Pu mass image vector, s. In the source→absorber→detector geometry used here, the Pu attenuation correction factor, CF, is given by

$$CF = \{\Sigma_e I_0(e) \cdot \exp(\mu_e)\}/\Sigma_e I_0(e) \ ,$$

$$\mu_e = \Sigma_z \rho_z \cdot U_{ez},$$

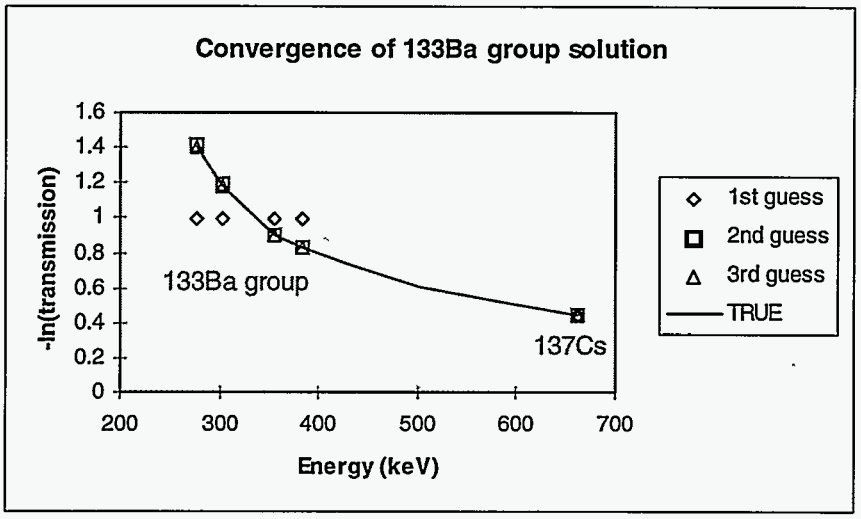

Figure 2. The rapid convergence of the estimated individual ^{133}Ba peak intensities in an energy-group-analysis iterative MBS fit. Although the initial guess for the ^{133}Ba transmissions is poor, the second guess is very close. By the third guess the estimated transmissions are within 0.5% of their true values.

where $I_0(e)$ is the unattenuated relative intensity of the e'th gamma ray peak in the group, ρ_z is the partial density of z'th basis material in the absorber, and U_{ez} is the attenuation coefficient for a standard amount of the z'th basis material at the e'th energy.

Figure 3 shows the ratio of the measured-to-true attenuation correction as a function of the transmission of the ^{239}Pu 414-keV gamma ray (measured with the HPGe detector) through the set of absorbers in Table II. The attenuation corrections estimated using the NaI detector with the linear continuum subtraction method were applied to the Pu transmissions measured with the HPGe detector (at 414-keV) and to the NaI detector (322- to 452 keV group net area, estimated using linear continuum subtraction). We can conclude from the figure that the net area method applied to NaI spectra gives good accuracy in determining attenuation corrections, but that the Pu peak net areas are less accurate and become completely unreliable at transmissions of less than 10%. To put the results in figure 3 in perspective, the standard deviation in the measured-to-true correction factor ratio was 3.5% when using HGPe data exclusively, 4.4% using Nai transmission

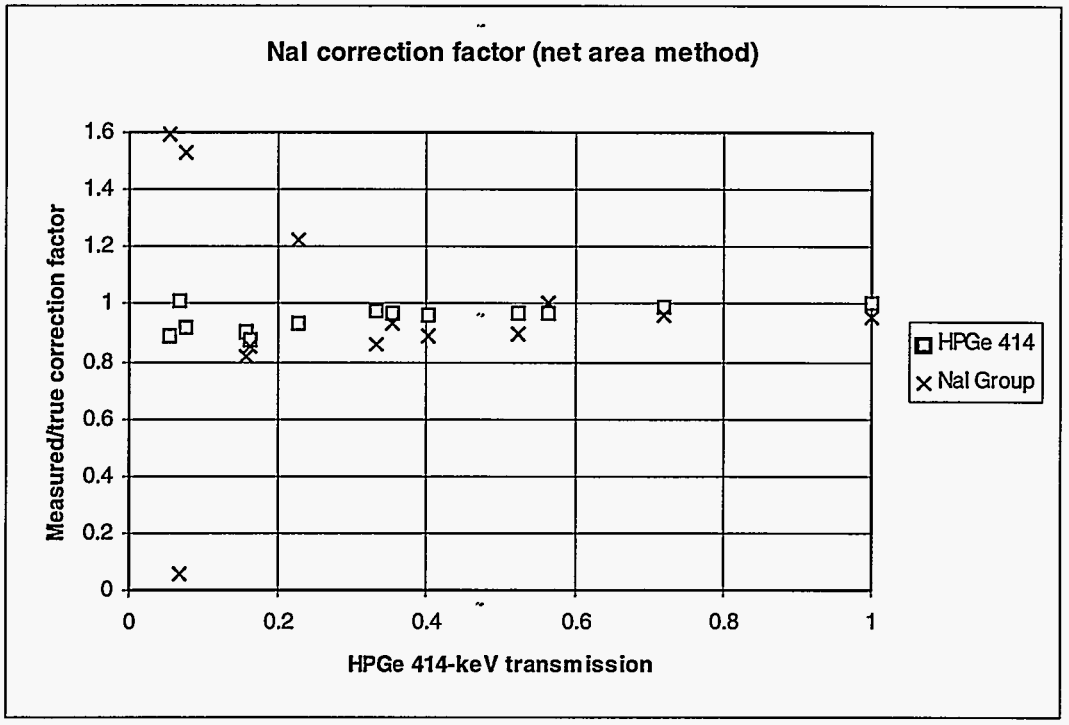

Figure 3. The measured-to-true attenuation correction as a function of the transmission of the ^{239}Pu 414-keV gamma ray (measured with the HPGe detector) through absorbers of varying composition and thickness. The attenuation corrections estimated using the NaI detector with the linear continuum subtraction method were applied to the Pu transmissions measured with the HPGe detector (at 414-keV) and to the NaI detector (322- to 452 keV group net area, estimated using linear continuum subtraction).

results to correct HPGe Pu emission data, and 11.5% (excluding points below 10% transmission) for using the net area NaI data for both.

AN EMPIRICAL RESPONSE FUNCTION APPROACH

We examined a simple empirical response function method that applies the MBS method directly to spectra rather than to transmissions computed from net peak areas. In this approach reference spectra of each transmission and emission source are measured after passing through air and through a set a basis materials and are then converted to logarithmic form to be used as a basis spectrum set. When the spectra of transmission

gamma-rays passing through an arbitrary absorber are decomposed into component basis spectra, the coefficients in the decomposition are the partial densities (ρ_z). These are equivalent to the ρ_z values determined using net peak areas and can be used without modification to correct HPGe or NaI net area emission data.

A similar response function technique can be applied to emission spectra of Pu. In this approach the ρ_z values are used to create a 'corrected' Pu spectrum. This spectrum represents the Pu spectrum that would have been obtained with no intervening absorbers, and in principle will have the same shape as the Pu reference spectrum through air but an amplitude that is proportional to the Pu mass. This is in fact a gross count technique. The only subtractions required (explicitly or implicitly as part of the fit procedure) are of the ambient background and of the rate-loss-source spectrum if one is used.

Side scattering must be treated in order to get accurate results in either the transmission or emission part of the problem. We used representative side-scattering spectra as a third MBS "material" for both parts of the problem. In the transmission method the solution vector becomes $\rho = [\rho_{Pb}, \rho_{CH2}, \rho_{scat}]^T$, where ρ_{scat} gives the amplitude of the scatter component. To subsequently use ρ to compute attenuation corrections for HPGe or NaI net-area emission data the ρ_{scat} component can be ignored. To compute corrections in the emission response function method, ρ_{scat} is used as the amplitude of the scatter component in the Pu spectrum. Although the ρ_{scat} component is subtractive when fitting the transmission data, applying the correction to the emission data is not. This is true even when using several scatter-component spectra. One can say that if the ρ vector is determined with good accuracy and precision in the transmission part of the problem, then the scatter components in the Pu spectrum become useful tidbits of information that add counts to the assay and improve assay sensitivity.

Transmission analysis with MBS response spectra

Let $\{\mathbf{c}_z\}$ be a set of composite spectra measured after transmission through each of n_z basis materials. By composite we mean that if separate spectra are taken for different

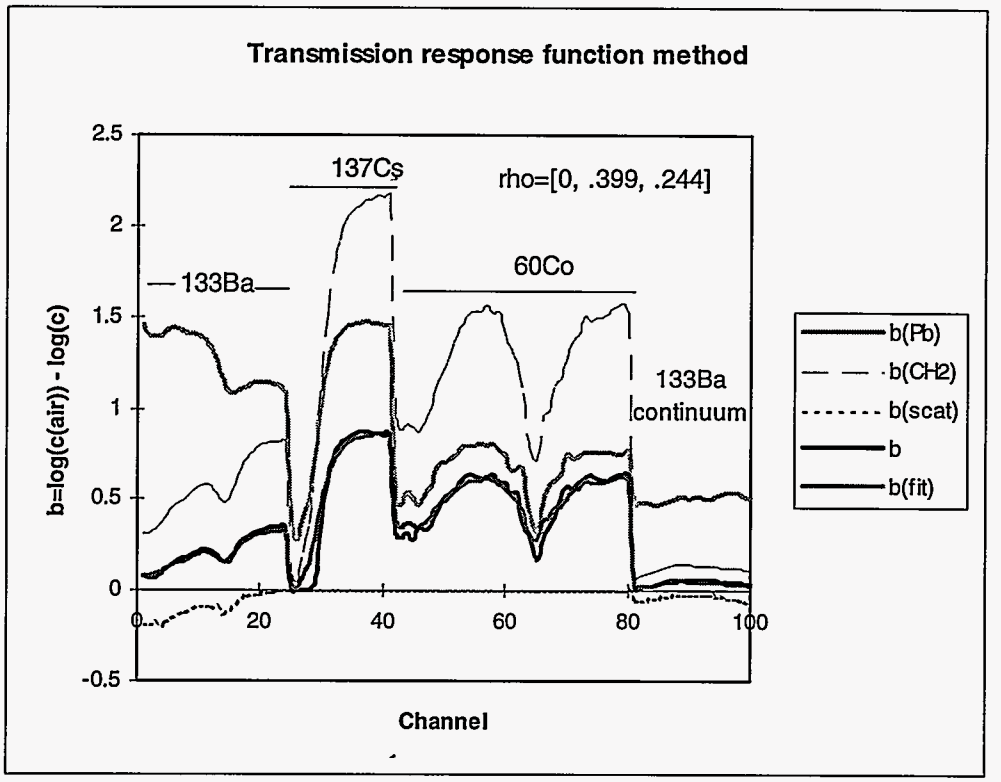

Figure 4. Illustration of the response function method applied to the composite transmission spectrum (**c**) for a 1.75-inch Al absorber. The logarithmic basis spectra are for 0.5-inches of Pb [**b**(Pb)], 10-inches of polyethylene [**b**(CH2)], plus a negative scatter component [**b**(scat)]. The best-fit combination of the basis functions to the curve **b** is given by **b**(fit) = 0 · **b**(Pb) + .399 · **b**(CH2) + .244 · **b**(scat), where the coefficients are the MBS ρ_z values for this basis set. The physical interpretation is that 1.75-inches of Al has attenuation properties equivalent to 3.99 inches of polyethylene, which is approx. true for gamma rays of these energies.

transmission sources, the interesting portions of each are extracted and arranged together into a single "spectrum" of counts. Figure 4 shows reference composite NaI spectra (in logarithmic form) created from separate ^{133}Ba, ^{137}Cs, and ^{60}Co sources transmitted through air and through our two basis absorbers (10-inches of polyethylene and 0.5-inch of Pb). The composite spectra contain the two ^{60}Co and the single ^{137}Cs peak, and the unresolved 276- to 384-keV peak group in ^{133}Ba. At the high end of the spectrum is a

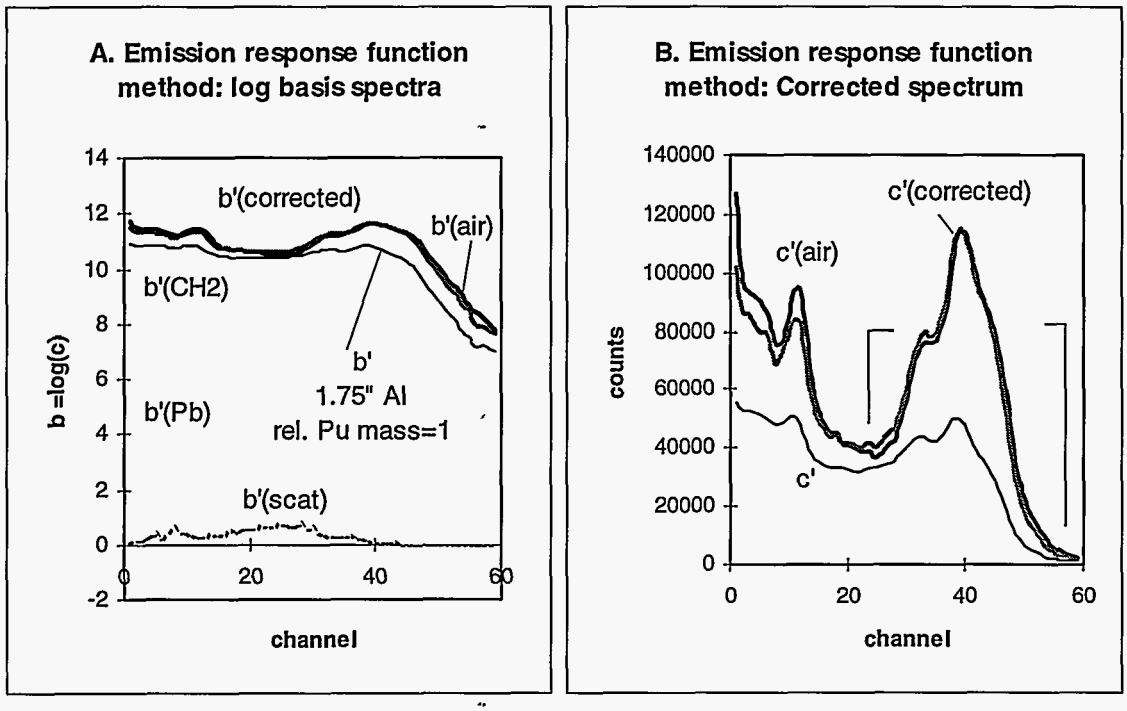

Figure 5. Illustration of the gross count response function method applied to the 100-g Pu source spectrum (**c'**) after passing through a 1.75-inch Al absorber. The ρ_z values determined for the transmission fit to the same absorber (see figure 4) were used to create the corrected log spectrum, **b'**(corrected), which was converted to the normal corrected spectrum, **c'**(corrected). (a) Log spectra, including the basis spectra **b'**(Pb), **b'**(CH2), **b'**(scat), and **b'**(air). (b) Linear scale transmission spectra. The lines show the summation region used.

scaled-down portion of the lower-energy continuum from ^{133}Ba. The scaling of the different spectrum components determines their weight in least squares fits.

To construct basis spectra ($\mathbf{b}_{Pb}$, $\mathbf{b}_{CH2}$) we make the conversion

$$b_{Pb,i} = \log(c_{air,i}) - \log(c_{Pb,i}) \ ,$$

and

$$b_{CH2,i} = \log(c_{air,i}) - \log(c_{CH2,i}) \ ,$$

where $c_{air,i}$, $c_{CH2,i}$, and $c_{Pb,i}$ are the (normalized) counts in the i'th channels in the air, CH_2, and Pb transmission spectra, respectively. Figure 4 shows these logarithmic basis spectra. A spectrum **c** taken through an arbitrary absorber must be similarly converted to a logarithmic spectrum, **b**, i.e.,

$$b_i = \log(c_{air,i}) - \log(c_i) \quad .$$

The 3-material MBS solution vector ρ (=$[\rho_{Pb}, \rho_{CH2}, \rho_{scat}]^T$) is computed by solving the linear system of equations

$$\mathbf{b} = U \cdot \rho \quad , \qquad (1)$$

where U is an N by 3 matrix whose columns are the N-channel spectra $\mathbf{b}_{Pb}$, $\mathbf{b}_{CH2}$, and $\mathbf{b}_{scat}$. We used the non-negative least squares (NNLS) fit option in TGS_FIT software to solve equation (1).

Figure 4 also shows fit results for a composite spectrum **b** measured through 1.75 inches of Al. The MBS solution was found to be $\rho = [\rho_{Pb}, \rho_{CH2}, \rho_{scat}]^T = [0, .399, .244]^T$. The physical meaning of this solution is that the absorber behaves like a material composed of (0)·(.5) = 0.0 inches of Pb and (0.399)·(10) = 3.99 inches of polyethylene, which is approximately correct for the energies involved.

Emission analysis with MBS response spectra

Figure 5a shows the basis spectra used for constructing a corrected Pu emission spectrum from the MBS partial density vector, ρ, determined by the response function method applied to the transmission data. The corrected Pu spectrum, $\mathbf{c'}_{corrected}$, and log spectrum, **b'**, are given by

$$\mu'_i = \rho_{Pb} \cdot b'_{Pb,i} + \rho_{CH2} \cdot b'_{CH2,i} + \rho_{scat} \cdot b'_{scat,i}$$

$$c'_{corrected,i} = \exp(\mu'_i) \cdot c'_i,$$

$$b'_{z,i} = \log(c'_{z,i}) ,$$

$$z = Pb, CH_2, \text{ or scat,}$$

where the c'_z are the basis spectra for Pu and b'_z are the corresponding logarithmic spectra. The Pu mass (with whatever isotopic composition is represented by the basis spectra) is given by

$$\text{mass(Pu)} = \text{mass(reference)} \cdot \Sigma_i \, c'_{corrected,i} / \Sigma_i \, c'_{air,i} \qquad (2)$$

where "mass(reference)" is the mass of Pu represented by the basis spectra and $\mathbf{c}'_{air}$ is the Pu reference spectrum with no attenuation. The summations are all over the same range, which in this study was limited to the upper part of the spectrum bracketing the 332- to 452-keV peak group, as shown by the lines in figure 5b. Note that because mass(Pu) here equals mass(reference) (they are the same source), the spectra **c**'(air) and **c**'(corrected) have the same amplitude.

As a matter of general interest, the Pu mass can be estimated for the simple source→absorber→detector geometry without using transmission sources by solving equation (1) for the Pu emission spectrum in the same manner as for transmission spectra, but with a constant term added to the basis set. That is, one uses the unit spectrum ($b_{unit,i}$ = 1, all i) as an additional basis spectrum. The amplitude ρ_{unit} of this constant term will be equal to the Pu mass relative to the reference mass.

Response function method results

Figures 6 and 7 show the results of applying the response function method to the series of absorbers in Table II. The results for correcting the HPGe detector 414-keV

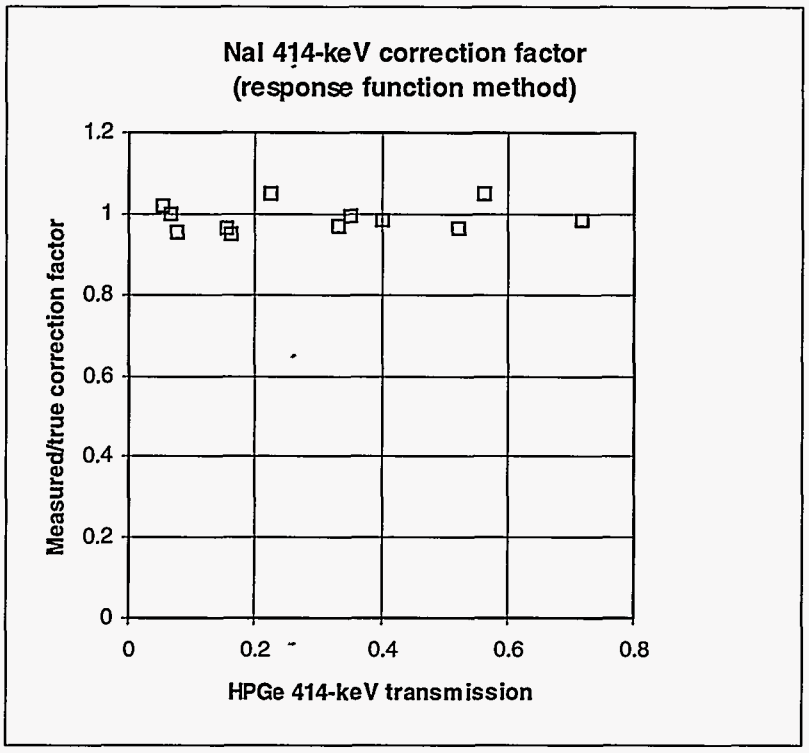

Figure 6. The measured-to-true attenuation correction as a function of the transmission of the 414-keV gamma ray through absorbers of varying composition and thickness. The attenuation corrections were measured using a NaI detector (response function method) and projected to 414 keV. The 'true' values were measured for the 414-keV gamma ray in ^{239}Pu using an HPGe detector.

gamma ray using the NaI transmission MBS solution are shown in Fig. 6. The results for correcting the NaI Pu gross spectrum using the same ρ are shown in Fig. 7. In figure 7, the results with and without the inclusion of side scattering are compared. The results are quite good overall, with a maximum mass error of only 3.5% when sidescattering is included.

SUMMARY AND CONCLUSIONS

Table III summarizes our results as the average mass (relative to the true value) and standard deviation of the estimated masses in the absorber series for each of the analysis methods condidered. The main conclusion we can draw is that all the methods

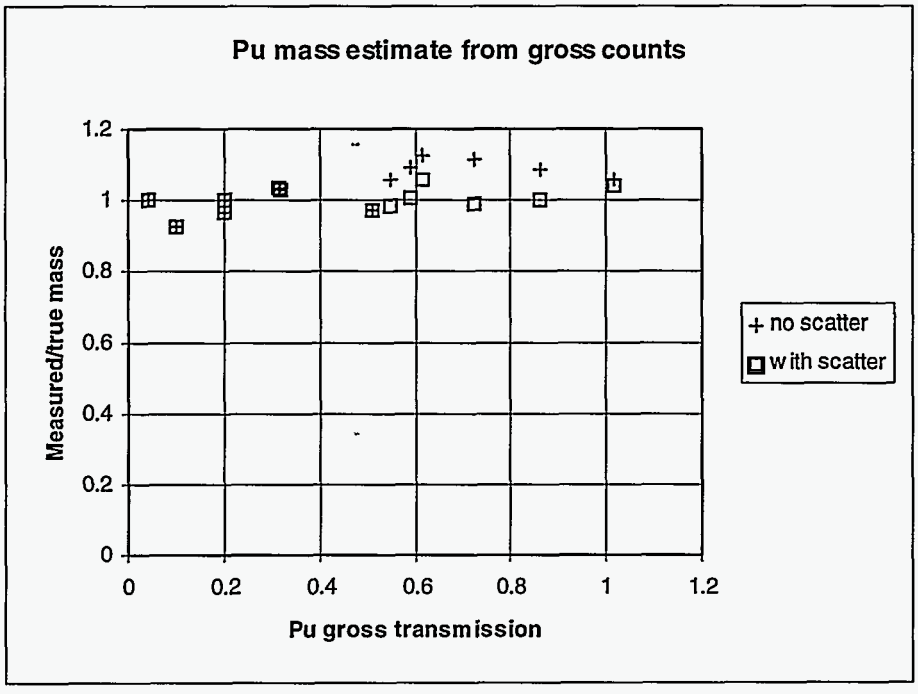

Figure 7. Pu mass estimate for a metallic 100-g Pu source transmitted through a range of materials. The masses were estimated using the empirical response function method for both the transmission and emission halves of the problem. Side scatter is ignored in the estimates plotted as '+' symbols, and is included in the estimates plotted as squares.

TABLE III. Summary of analysis results

Transmission source analysis method	Emission source (Pu) analysis method	Average estimated/true mass	Standard deviation (relative)
HPGe	HPGe	1.007	3.5%
NaI, continuum subtraction	HPGe	.95	4.4
NaI, continuum subtraction	NaI, continuum subtraction	.94*	11.5*
NaI, response function	HPGe	.990	3.4%
NaI, response function	NaI, response function	1.001	3.5%

*for transmissions >= 10%

studied worked well except for the linear continuum subtraction in Pu spectra. The problem in that case is that the Pu peak areas are not accurately extracted with linear continuum subtraction (the method worked well on the transmission peaks). It seems likely that more refined net area determinations (e.g., using a response function approach) will give good results.

NaI detectors worked very well when using the gross count response function method, but there are two important caveats concerning their application to TGS and SGS. The first is that the method requires accurate Pu response functions to give the best accuracy. This implies that the isotopic composition of the waste is well known . The second caveat is that we do not know yet how well the treatment of the scattered components will translate from the simple geometry studied here to TGS systems. If the method does not translate well, the scattered components will have to be treated using a response function analysis on the Pu spectra, which would introduce a subtractive element that would degrade the sensitivity. Even so, we believe that the dramatic improvement in sensitivity, along with the ability to image at higher resolutions without increasing the scan time, make NaI arrays an attractive option for the next generation of TGS systems.

REFERENCES

1) R.J. Estep, T.H. Prettyman, and G.A. Sheppard, "Tomographic gamma scanning to assay heterogeous radioactive waste," Nucl. Sci. and Eng. **118**, 145-152.
2) R.J. Estep, T.H. Prettyman, and G.A. Sheppard, "Comparison of atteuation correction methods for TGS and SGS: Do we really need selenium-75?" Proc. 37th annual INMM meeting, Naples, FL (July, 1996).
3) R.J. Estep, T.H. Prettyman, and G.A. Sheppard, "Reduction of TGS image reconstruction times using separable attenuation coefficient models," ANS Winter Meeting, San Francisco, CA (June 15, 1995). Also, Los Alamos Rept LA-UR-95-2013.
4) R.J. Estep, "TGS_FIT 3.0: Image reconstruction software for quantitative, low-resolution tomographic assays," to be published, Los Alamos National Lab.
5) R.J. Estep, "TGS_FIT: Image reconstruction software for quantitative, low-resolution tomographic assays," Los Alamos National Lab report, LA-12497-MS (1993).